



The Thomas Jefferson National Accelerator Facility
Theory Group Preprint Series

JLAB-THY-99-23

New Modes: $D_s^+ \rightarrow \rho^+ \gamma$, $D^+ \rightarrow K^{*+} \gamma$, and Weak Annihilation

Richard F. Lebed

Jefferson Lab, 12000 Jefferson Avenue, Newport News, VA 23606

(August, 1999)

Additional copies are available from the authors.

The Southeastern Universities Research Association (SURA) operates the Thomas Jefferson National Accelerator Facility for the United States Department of Energy under contract DE-AC05-84ER40150.

Abstract

A class of decay modes sensitive to only one quark topology at leading G_F order (annihilation of valence quarks through a W) is described. No experimental observations, nor even upper limits, have been reported for these decays. This work presents a simpleminded (order-of-magnitude) first calculation of their branching fractions. Although rare, one of these modes ($D_s^+ \rightarrow \rho^+ \gamma$) might already be observable at charm experiments, while another ($D^+ \rightarrow K^{*+} \gamma$) should appear at the B factories, and the rest at hadron colliders.

13.25.Ft, 13.40.Hq, 13.25.Jx

DISCLAIMER

This report was prepared as an account of work sponsored by the United States government. Neither the United States nor the United States Department of Energy, nor any of their employees, makes any warranty, expressed or implied, or assumes any legal liability or responsibility for the accuracy, completeness, or usefulness of any information, apparatus, product, or process disclosed, or represents that its use would not infringe privately owned rights. Reference herein to any specific commercial product, process, or service by trade name, mark, manufacturer, or otherwise, does not necessarily constitute or imply its endorsement, recommendation, or favoring by the United States government or any agency thereof. The views and opinions of authors expressed herein do not necessarily state or reflect those of the United States government or any agency thereof.

I. INTRODUCTION AND MOTIVATION

As data on charm and beauty decays accumulates at CLEO, BES, and the Fermilab and LEP experiments, and soon at the B factories BABAR and BELLE, it becomes possible to study ever more rare decays in search of interesting and exotic physics. This work suggests examining a previously neglected class, electromagnetic decays of a charged meson mediated by the weak annihilation of the meson. Such decays are indeed rare, with branching fractions suppressed by α , not to mention the difficulty of forcing a camel (the whole meson wavefunction) through the eye of a needle (the pointlike W vertex multiplied by CKM factors), but their branching fractions need not be so tiny as one might think.

Let us focus upon processes with only one meson in the final state. Such decays are especially interesting because they proceed through only one weak decay topology at leading order in G_F if the flavors of the quarks in the final state and those in the initial state are distinct, and if the initial and final quark have the same electric charge (and similarly for the antiquarks). This is the s -channel annihilation topology presented in Fig. 1. Note that the first condition requires each valence quark to terminate on a flavor-changing vertex, while the second eliminates the possibility of a t -channel W exchange. The photon may be attached to any charged line, although of course couplings to the lighter constituents are favored. At $O(G_F^2)$ corrections enter through diagrams with a penguin loop on each of the quark and antiquark lines (Fig. 2a) and crossed-box diagrams (Fig. 2b), neither of which is expected to be very large. In addition, one may go beyond the valence diagrams and describe the weak process including its short-distance QCD corrections in terms of operators mixed through evolution of the corresponding anomalous dimension matrix, but we do not perform this refinement in this work.

The interest in such decays lies partly in the simplicity of the weak topology and sensitivity to a number of hard-to-isolate CKM elements as well as strong and electromagnetic matrix elements on one hand, and the simplicity of the two-body final state on the other. Indeed, the hard, monochromatic final-state photon should prove an exceptionally unambiguous experimental signal for these decays. It should also be pointed out that these modes would represent the first electromagnetic decays observed for the charged 0^- mesons D^+ , D_s^+ , B^+ , or B_c^+ .

The first such decays studied [1], $B^+ \rightarrow D_s^{*+}\gamma$ and $D^{*+}\gamma$ (generically, $D_{(s)}^{*+}\gamma$), were suggested as probes of $|V_{ub}|$ and were estimated to have rates of approximately 2×10^{-7} and 7×10^{-9} , respectively. A number of the theoretical uncertainties associated with these estimates can be eliminated if the on-shell photon is replaced by an $\ell^+\ell^-$ pair [2], and the invariant mass q^2 of the virtual photon is used to define an operator product expansion. The price one pays for this improvement is an extra factor of α , so that such decays are estimated to have branching fractions of a few times 10^{-10} or 10^{-12} , depending upon the level of Cabbibo suppression. The t -channel exchange processes mentioned above, which have neutral initial- and final-state mesons, are discussed in [3], and yield similar branching ratios. Most of these processes are too rare to be seen in appreciable numbers at the B factories (with combined yields of some millions of B^+B^- pairs per year [4]), but may be observable at hadron collider experiments.

The B decays are beset with an additional suppression in the form of an especially small CKM factor. Table I presents decays representing the 6 possible weak annihilation flavor

assignments, along with the CKM factors in the amplitude and their behavior in powers of the Wolfenstein parameter $\lambda \approx 0.22$. We see that the B decays suffer from the worst CKM suppressions, and thus focus on the other modes. Especially interesting are the Cabbibo-unsuppressed mode $D_s^+ \rightarrow \rho^+\gamma$, which we shall estimate to have a branching fraction of nearly 10^{-4} and might already appear in charm experiment data, and the doubly-Cabbibo suppressed mode $D^+ \rightarrow K^{*+}\gamma$ with a branching fraction perhaps as large as 10^{-6} , which exhibits a neutrinoless decay proportional to $|V_{cs}|^2$ at leading order in G_F .

The rest of this paper is organized as follows: In Sec. II, we present a very simple-minded calculation of the rate for these processes and a list of approximations used, while Sec. III presents numerical results, outlines experimental prospects for the observation of these modes, lists potential theoretical improvements, and concludes.

II. CALCULATION

The calculation presented in this section is very simplistic, in that it relies on a number of substantial approximations made explicit below. However, it is significant not in providing an exact determination of widths and branching ratios, but in obtaining the order of magnitude of these quantities as an estimate for experimenters searching for signals of these modes, and as a point of comparison for theorists performing subsequent, more refined calculations.

The generic process we consider is $M \rightarrow P \rightarrow V\gamma$, where M is the massive initial 0^- state, P is a lighter virtual 0^- meson with the flavor quantum numbers of the final state, and V is the final-state 1^- meson, as depicted in Fig. 3. In modeling the decay this way, we make the following assumptions:

1. Photon emission from M is neglected, so the process $M \rightarrow M^*\gamma \rightarrow V\gamma$ is not included, as was done in Ref. [1]. In the previous calculation, where $M = B^+$, $M^* = B^{*+}$, $P = D_{(s)}^+$, and $V = D_{(s)}^{*+}$, the $MM^*\gamma$ and $PV\gamma$ couplings were related through heavy quark spin-flavor symmetry (HQSF), and both diagrams were included. However, in the current case with, for example, $V = K^{*+}$ or ρ^+ , this is no longer an acceptable approximation, and we include only the photon coupling to the lighter mesons. This assumption likely leads to an underestimate of the branching ratio, but probably not an exceptionally large one: The K^{*+} and ρ^+ electromagnetic widths are 50 ± 5 and 68 ± 7 keV, respectively, while that of the D^{*+} is less than 4.2 keV.¹
2. Complete factorization with vacuum insertion approximation is assumed for the weak vertex. The annihilation of M and the creation of P are assumed to occur at a single point. This approximation neglects both the short-distance QCD corrections as mentioned above, and long-distance hadronic contributions. As an example of the latter, the initial weak vertex may, rather than annihilating the initial meson, produce a quark (or antiquark) q that is the antiparticle of one of the meson valence quarks,

¹Nonetheless, one should note that a small propagator denominator ($m_V^2 - m_{M^*}^2$) or different a light quark charge in M^* can enhance the importance of such couplings in the full width.

and this four-quark intermediate state propagates for some time before $q\bar{q}$ annihilation occurs. Specifically, processes like $D^+ \rightarrow (K^+\pi^0 \text{ or } K^0\pi^+) \rightarrow K^{*+}\gamma$ are not included.

3. The intermediate state P is assumed to be the lightest pseudoscalar with the same flavor quantum numbers as the final-state V . Certainly many other resonant as well as multiparticle states can couple the weak vertex to $V\gamma$.² The present assumption is made partly because data exists on the $PV\gamma$ coupling from the observed decay $V \rightarrow P\gamma$, and partly because the lightest pseudoscalar P among all possible intermediates presumably has the one of the largest couplings to $V\gamma$. In any case, this approximation leads to an underestimate of the correct branching ratio.
4. In relating the virtual process $P \rightarrow V\gamma$ to the on-shell $V \rightarrow P\gamma$, one relates the single (magnetic) form factor $\mathcal{C}(q^2)$ at a virtuality of $q^2 = M_M^2 - m_P^2$ to that at $q^2 = 0$. We take them numerically equal, although this tends to overestimate the rate, since form factors tend to fall off away from $q^2 = 0$. Nevertheless, we indicate this ratio explicitly in the final expression, see Eq. (2.4) below.

Given these assumptions, the calculation of the rate is a simple matter. The weak mixing vertex, mediated by an operator \mathcal{O}_W , in vacuum insertion approximation is given by

$$\begin{aligned}
& \langle P(p_M) | \mathcal{O}_W | M(p_M) \rangle \\
&= -i \frac{G_F}{\sqrt{2}} V_P V_M B \langle P(p_M) | \bar{Q}_P \gamma^\mu (1 - \gamma_5) q_P | 0 \rangle \langle 0 | \bar{q}_M \gamma_\mu (1 - \gamma_5) Q_M | M(p_M) \rangle \\
&= -i \frac{G_F}{\sqrt{2}} V_P V_M B (-i f_P p_M^\mu) (+i f_M p_{M\mu}) \\
&= -i \frac{G_F}{\sqrt{2}} V_P V_M f_P f_M M^2 B,
\end{aligned} \tag{2.1}$$

where M_M is now abbreviated as M , the valence structure of P is $Q_P \bar{q}_P$, that of M is $Q_M \bar{q}_M$, and $V_{M,P}$ are the CKM parameters associated with the annihilation of M and creation of P , respectively. We also allow for a coefficient B parameterizing the incompleteness of the vacuum saturation approximation, as in $\bar{B}B$ mixing, but set it to unity in our numerical estimates. The intermediate 0^- state P provides the simple propagator $i/(p_M^2 - m_P^2)$. The photon vertex is extracted from the decay $\Gamma_{V \rightarrow P\gamma}$, which has invariant amplitude

$$\mathcal{M} = \mathcal{C}(p_P^2 - m_P^2) \epsilon_{\mu\nu\rho\sigma} \epsilon_V^\mu \epsilon_\gamma^\nu p_P^\rho p_V^\sigma, \tag{2.2}$$

where the Lorentz coupling is determined in part by the 0^- quantum number of P . \mathcal{C} is a magnetic form factor, and simply becomes a transition magnetic moment when its momentum transfer argument $p_P^2 - m_P^2$ is set to zero in the on-shell case. The rate obtained from this amplitude is

²However, a single vector intermediate is not permitted because the initial-state matrix element in the factorization approximation couples as $f_M p_M^\mu$, $p_M = p_P$, and a vector P couples as ϵ_P^μ , giving an inner product that vanishes due to transversality.

$$\Gamma_{V \rightarrow P\gamma} = \frac{1}{12\pi} \mathcal{C}^2(0) E_\gamma^3. \tag{2.3}$$

The full rate for $M \rightarrow V\gamma$ also uses \mathcal{C}^2 , but now has the argument $M^2 - m_P^2$. For our numerical estimates, we assume that \mathcal{C} does not change dramatically over this range, and use data on $\Gamma_{V \rightarrow P\gamma}$ to eliminate \mathcal{C} from the expression for $\Gamma_{M \rightarrow V\gamma}$; however, since this is certainly a contentious approximation, we formally retain the ratio of \mathcal{C} at the two different argument values in the full expression for the width. Putting this together, one obtains our central result:

$$\begin{aligned}
\Gamma(M \rightarrow V\gamma) &= \frac{3}{2} G_F^2 |V_M V_P|^2 f_M^2 f_P^2 B^2 \Gamma_{V \rightarrow P\gamma} \left[\frac{\mathcal{C}(M^2 - m_P^2)}{\mathcal{C}(0)} \right]^2 \\
&\times \left(\frac{M^2}{M^2 - m_P^2} \right)^2 \left(\frac{M^2 - m_V^2}{m_V^2 - m_P^2} \right)^3 \left(\frac{m_V}{M} \right)^3.
\end{aligned} \tag{2.4}$$

Here, the cubed mass factors are nothing more than the ratio of E_γ^3 for $M \rightarrow V\gamma$ to that for $V \rightarrow P\gamma$.

One may compare Eq. (2.4) to Eq. (17) of Ref. [1] for $B^+ \rightarrow D_{(s)}^+ \gamma$, which in the current notation reads

$$\begin{aligned}
\Gamma(M \rightarrow V\gamma) &= \frac{27}{8} G_F^2 |V_M V_P|^2 f_M^4 B^2 \Gamma_{V' \rightarrow P'\gamma} \left[\frac{\mathcal{C}(M^2 - m_P^2)}{\mathcal{C}(0)} \right]^2 \\
&\times \left[\frac{m_V M (M - m_V) (M + m_V)^3}{(m_{V'}^2 - m_P^2)^3} \right] \left(\frac{m_{V'}}{M} \right)^3,
\end{aligned} \tag{2.5}$$

where the $0^-, 1^-$ pair P', V' are related to P, V by HQS: The primed mesons are introduced when data for $\Gamma_{V \rightarrow P\gamma}$ is unavailable. In Ref. [1], P', V' were D^+, D^{*+} ; the current calculation uses only information from the unprimed mesons directly, so $P', V' \rightarrow P, V$ here. All of the differences between Eqs. (2.4) and (2.5) can be accounted for by the assumptions of HQS: First, the magnetic moment form factors for all heavy mesons were assumed the same, except for a trivial coefficient due to the electric charge $Q_{q(m)}$ of the lighter quark q in the meson m to which the photon couples. Since both the $MM^*\gamma$ and $PV\gamma$ couplings were included in the HQS calculation, an extra enhancement of $(Q_{q(M)} + Q_{q(V)})^2 / Q_{q(V)}^2$, a factor of 9, appeared in Ref [1]. Next, in HQS one has $f_M^2 M = f_P^2 m_P$, and $m_V - m_P = O(1/M)$, M being the heavy quark mass. The remaining differences arise from the fact that fields containing heavy quarks in HQS are nearly static, even if the heavy quark changes flavor. This leads one to adopt the normalization of HQS states of 1 rather than $2M$ particles per unit volume, as well as introduce propagators linear rather than quadratic in particle masses, and these modifications often lead to effective lowest-order substitutions (in the current notation) such as $(M + m_V)/2 \rightarrow M$. Equations (2.4) and (2.5) are related by the application of these properties.

III. RESULTS AND CONCLUSIONS

We use Eq. (2.4) to obtain branching fraction estimates for the last four modes exhibited in Table I (the first two are discussed in Ref. [1] using Eq. (2.5)). We use standard *Review of*

Particle Physics (RPP) [5] values for masses, decay constants, CKM elements, and lifetimes whenever possible, with the following exceptions: We take $|V_{cb}| = 3 \times 10^{-3}$ and $f_D = f_{D_s} = 200$ MeV. Following recent experiments, we use the E791 value [6] $\tau_{D_s} = 0.518 \pm 0.014 \pm 0.007$ psec, and the CDF values [7] $m_{B_c^+} = 6.40 \pm 0.39 \pm 0.13$ GeV, $\tau_{B_c^+} = 0.46_{-0.16}^{+0.18} \pm 0.03$ psec. OPAL [8] and ALEPH [9] have also reported a few B_c candidate events, with mass values consistent with [7]. We also use the HQS relation to obtain $f_{B_c} \approx f_B \sqrt{m_B/m_{B_c}} \approx 155$ MeV. As mentioned previously, we take $B^2 = 1$ and $C^2(M^2 - m_p^2)/C^2(0) = 1$.

The resulting branching fractions are exhibited in Table II, along with the energies of the final-state photon. From these numbers, we see that the B_c^+ modes are rare but not exceptionally so; of course, the B factories are not designed to produce them anyway, so their possible observation must necessarily wait for the upcoming hadron collider experiments. A few $D^+ \rightarrow K^{*+}\gamma$ should appear each year at the B factories, with the exact number depending upon the correct value of the mantissa in our estimate. The mode $D_s^+ \rightarrow \rho^+\gamma$ might even be observable right now at charm experiments such as at BES if our estimate is low by a factor of a few, based on limits in the RPP [5]; in any case, they can place an upper limit on its branching fraction.

Although much physics is neglected in this simple calculation, our estimates show that weak annihilation decays may be observed in the near future. They are attractive from both the experimental and theoretical perspective. Improvement of the theoretical calculation essentially amounts to improving on the four assumptions made in Sec. II. Lifting the first requires new data for the heavy coupling in $M^* \rightarrow M\gamma$, particularly positive data for $D^{*+} \rightarrow D^+\gamma$. Improving the vacuum insertion approximation can be accomplished as in $\bar{B}B$ mixing, with lattice or model calculations, and including the short-distance QCD corrections is a straightforward matter. As for the remaining two assumptions, one can be freed of both the lowest-resonance dominance and constant form factor assumptions by carrying out for example, a light-cone or inclusive quark model calculation.

From the experimental side, it would be interesting to see what direct bounds can be placed on these modes at the current time, in anticipation of their eventual observation. Once observed, the weak annihilation modes will present an interesting probe of CKM elements, electromagnetic transitions, and meson wavefunctions.

Acknowledgments

I thank C. Carlson, C. Carone, and V. Sharma for useful discussions. This work is supported by the Department of Energy under contract No. DE-AC05-84ER40150.

REFERENCES

- [1] B. Grinstein and R. F. Lebed, Phys. Rev. D **60**, 031302(R) (1999).
- [2] D. H. Evans, B. Grinstein, D. R. Nolte, Phys. Rev. D **60**, 057301 (1999); Report No. UCSD/PTH 99-05, hep-ph/9904434 (unpublished).
- [3] D. H. Evans, B. Grinstein, D. R. Nolte, Report No. UCSD/PTH 99-05, hep-ph/9906528 (unpublished).
- [4] See, for example, *The BABAR Physics Book*, P. F. Harrison and H. R. Quinn, editors, Report No. SLAC-R-504, Stanford Linear Accelerator, Stanford, CA, 1998.
- [5] Particle Data Group (C. Caso *et al.*, *Review of Particle Physics*, Eur. Phys. J. C **3**, 1 (1998).
- [6] E791 Collaboration (E. M. Aitala *et al.*), Phys. Lett. B **445**, 449 (1999).
- [7] CDF Collaboration (F. Abe *et al.*), Phys. Rev. Lett. **81**, 2432 (1998).
- [8] OPAL Collaboration (K. Ackerstaff *et al.*), Phys. Lett. B **420**, 157 (1998).
- [9] ALEPH Collaboration (R. Barate *et al.*), Phys. Lett. B **402**, 213 (1997).

TABLES

Valence structure	Decay mode	CKM Elements
$b\bar{u} \rightarrow c\bar{s}\gamma$	$B^+ \rightarrow D_s^{*+}\gamma$	$V_{ub}^*V_{cs} \sim \lambda^3$
$\bar{b}u \rightarrow c\bar{d}\gamma$	$B^+ \rightarrow D^{*+}\gamma$	$V_{ub}^*V_{cd} \sim \lambda^4$
$\bar{b}c \rightarrow u\bar{s}\gamma$	$B_c^+ \rightarrow K^{*+}\gamma$	$V_{cb}^*V_{us} \sim \lambda^3$
$\bar{b}c \rightarrow d\bar{u}\gamma$	$B_c^+ \rightarrow \rho^{*+}\gamma$	$V_{cb}^*V_{ud} \sim \lambda^2$
$c\bar{d} \rightarrow u\bar{s}\gamma$	$D^+ \rightarrow K^{*+}\gamma$	$V_{cd}^*V_{us} \sim \lambda^2$
$c\bar{s} \rightarrow u\bar{d}\gamma$	$D_s^+ \rightarrow \rho^{*+}\gamma$	$V_{cs}^*V_{ud} \sim \lambda^0$

TABLE I. Flavor structure and mesonic decay modes of weak annihilation electromagnetic decays. The CKM coefficient for each process is accompanied by its magnitude in terms of Wolfenstein $\lambda \approx 0.2$.

Decay mode	Branching Ratio (est.)	Photon Energy (GeV)
$B_c^+ \rightarrow K^{*+}\gamma$	4×10^{-7}	3.14
$B_c^+ \rightarrow \rho^{*+}\gamma$	4×10^{-6}	3.15
$D^+ \rightarrow K^{*+}\gamma$	6×10^{-7}	0.72
$D_s^+ \rightarrow \rho^{*+}\gamma$	8×10^{-5}	0.83

TABLE II. Estimates of branching fractions for weak annihilation decays using Eq. (2.4). Also included are energies of the monochromatic photon.

FIGURES

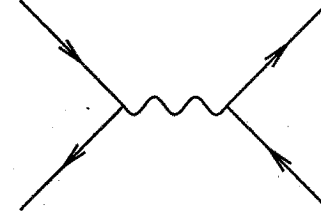


FIG. 1. The s -channel weak annihilation topology.

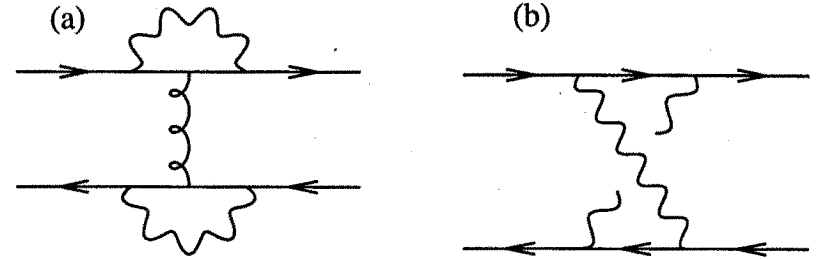


FIG. 2. $O(G_F^2)$ corrections to Fig. 1: (a) di-penguin diagram; (b) crossed-box diagram.

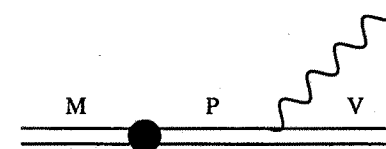


FIG. 3. Meson decay diagram for the process $M \rightarrow P \rightarrow V\gamma$. The blob represents the flavor-changing vertex of Fig. 1 and its corrections.